APME — Actualităţi şi Perspective în Domeniul Maşinilor Electrice
Electric Machines, Materials and Drives - Present and Trends
18, *1*, pp. 118–124, 2022

NUMERICAL ANALYSES ON THE RESPONSES OF UNIMORPH AND BIMORPH PIEZOELECTRIC HARVESTERS IN TIME DOMAIN

Yelda VELI[1], Claudia SĂVESCU[1,2], Alexandru MOREGA[1,3], Daniel COMEAGĂ[1]
[1] Faculty of Electrical Engineering, University Politehnica of Bucharest, Bucharest, Romania
[2] Romanian Research and Development Institute for Gas Turbines COMOTI, Bucharest, Romania
[3] "Gheorghe Mihoc–Caius Iacob" Institute of Statistical Mathematics and Applied Mathematics, Romanian Academy
yelda.veli@upb.ro, claudia.borzea@comoti.ro, amm@iem.pub.ro, daniel.comeaga@upb.ro

Abstract. The paper presents the assessment of the electric output rendered by a unimorph and a bimorph piezoelectric harvester, with one and two active piezoceramic wafers, using numerical simulations. Expected sinusoidal voltages were obtained in a time-dependent study, with a time step corresponding to the eigenfrequency found after conducting an Eigenfrequency study. The terminal voltages obtained agree with the Euler-Bernoulli beam theory and with the distance of the piezoelectric layers from the neutral fiber. By adding an electric circuit node to the electric field problem to form a closed internal circuit, a single unified sinusoidal voltage response should be obtained, coinciding with the input vibration signal. The independent voltages of the layers of a piezoelectric structure with more than one layer (usually two or four) cannot be observed experimentally, as a harvester has only two terminals that pick the overall electric response from all the layers, giving a single alternating voltage output.

Rezumat. Lucrarea prezintă evaluarea răspunsului electric al unui dispozitiv piezoelectric de recoltare a energiei unimorf și bimorf, cu unul și respectiv două plăcuțe piezoceramice active, prin intermediul simulărilor numerice. Au fost obținute tensiunile sinusoidale în studiul tranzitoriu, cu un pas de timp corespunzător frecvenței naturale găsite după efectuarea unui studiu de frecvențe proprii. Tensiunile la borne obținute sunt în conformitate cu teoria barei Euler-Bernoulli și cu distanța straturilor piezoelectrice de la fibra neutră. Prin adăugarea unui nod de circuit electric problemei de câmp electric, pentru a forma un circuit intern închis, ar trebui să se obțină un singur răspuns în tensiune sinusoidal unificat, care să coincidă cu semnalul de vibrație de intrare aplicat. Tensiunile independente ale straturilor unei structuri piezoelectrice cu mai mult de un strat (de obicei două sau patru straturi) nu pot fi observate experimental, deoarece un dispozitiv piezoelectric tip microgrindă în consolă dispune de doar două terminale care preiau răspunsul electric global de la toate straturile, dând o singură tensiune de ieșire sinusoidală.

1. INTRODUCTION

Piezoelectric energy harvesting is a thoroughly researched topic that has recently gained popularity. Numerous papers in the literature focused only on numerical simulations, analyses, and optimizations [1–9]. However, not many articles address the time response [10,11]. This is explained by the increased complexity, computational resources, and simulation time required by time-dependent study and some difficulties encountered in transient studies in the specific simulation program. Another aspect is that a transient analysis is often considered redundant to a frequency domain study, which most often suffices to assess the behavior of the piezoelectric harvester (PEH).

The paper addresses the sinusoidal voltage output of a unimorph and a bimorph piezoelectric cantilever with one and two piezoceramic layers. The simulation models aim to be applied to a real quadmorph PEH [12].

ISSN / ISSN-L: 1843-5912
https://www.doi.org/10.36801/apme.2022.1.14

The paper aims to assess the global and individual electric potentials rendered by each piezoelectric wafer. This cannot be seen in practice since the harvesters only have a pair of +/- terminals, which enter through the same BNC connector to the measuring device's input. Thus, a single unified sinusoidal voltage can only be observed experimentally.

2. SIMULATION MODEL

The simulated geometry was inspired by Mide PPA-4011 piezoelectric harvester (Fig. 1), which has been simulated and tested in previous research works [12–15]. The physical harvester has four PZT-5H layers and complicated internal circuitry regarding the electrical connections, which is not disclosed by the manufacturer [16]. For bimorph structures, the bottom wafer is usually poled opposite the top wafer, concerning the neutral axis in the center [17].

The electrical connections are then made with the two wafers connected in parallel, but in such a way that the two wafers always act in the opposite direction of one another (one compresses while the other elongates). This is the desired configuration when using these products as benders for energy harvesting [16].

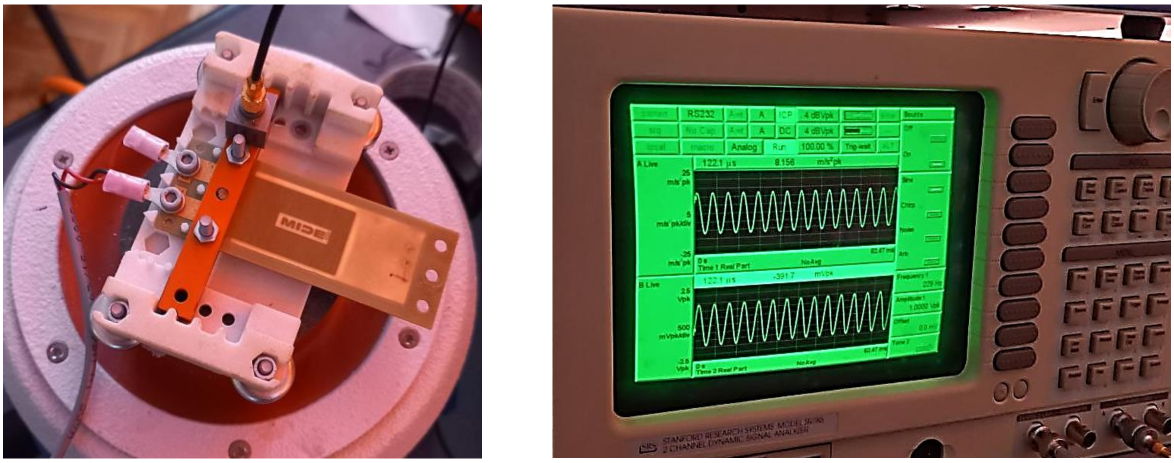

a) Piezoelectric harvester on shaker b) Spectrum analyser

Fig. 1 – Experimental setup of the piezoelectric harvester and the input sinusoidal signal measured by an accelerometer (upper channel A) and voltage time response (bottom channel B).

The simulations were conducted using the finite element method [18]. The numerical analysis is based on the piezoelectric constitutive relations in the strain-charge form:

$$\begin{cases} \mathrm{S} = \mathrm{s_E T} + \mathrm{d^T E} \\ \mathrm{D} = \mathrm{dT} + \varepsilon_\mathrm{T} \mathrm{E} \end{cases}, \tag{1}$$

where: **S** [ND] – strain; s_E [1/Pa] – elastic compliance, T [N/m^2] – stress; d^T [C/N] – piezoelectric charge constant, E [V/m] – electric field strength, D [C/m^2] – electric displacement, ε_T [F/m] – electric permittivity, at constant stress.

The electric field laws on which the software computes the electrostatics physics are consequences of Faraday's law (2), electric flux law (3), conduction law (4), and electric charge conservation law (5).

$$\mathbf{E} = -\nabla \mathbf{V}, \tag{2}$$

$$\nabla \cdot \mathbf{D} = \boldsymbol{\rho}_\mathbf{V}, \tag{3}$$

$$\mathbf{J} = \boldsymbol{\sigma} \mathbf{E}, \tag{4}$$

$$\nabla \cdot \mathbf{J} = \mathbf{0}, \tag{5}$$

where: **E** [V/m] – electric field strength; V [V] – electric potential, **D** [C/m^2] – electric displacement; **J** [A/m^2] – electric current density, ρ_V [V] – electric charge density; σ [S/m] – electric conductivity. An extra relation is added for piezoelectric charge conservation to include the polarization vector **P** [C/m^2]:

$$\boldsymbol{D} = \boldsymbol{\varepsilon_0 E} + \boldsymbol{P}. \qquad (6)$$

The simplified geometry with all the constitutive parts is shown in Fig. 2. The BCs used for the electric field problem is presented in Fig. 2,b, for the unimorph PEH, and in Fig. 2,c, for the bimorph PEH. The BC used for the mechanical problem is indicated in Fig. 2,a with a green arrow.

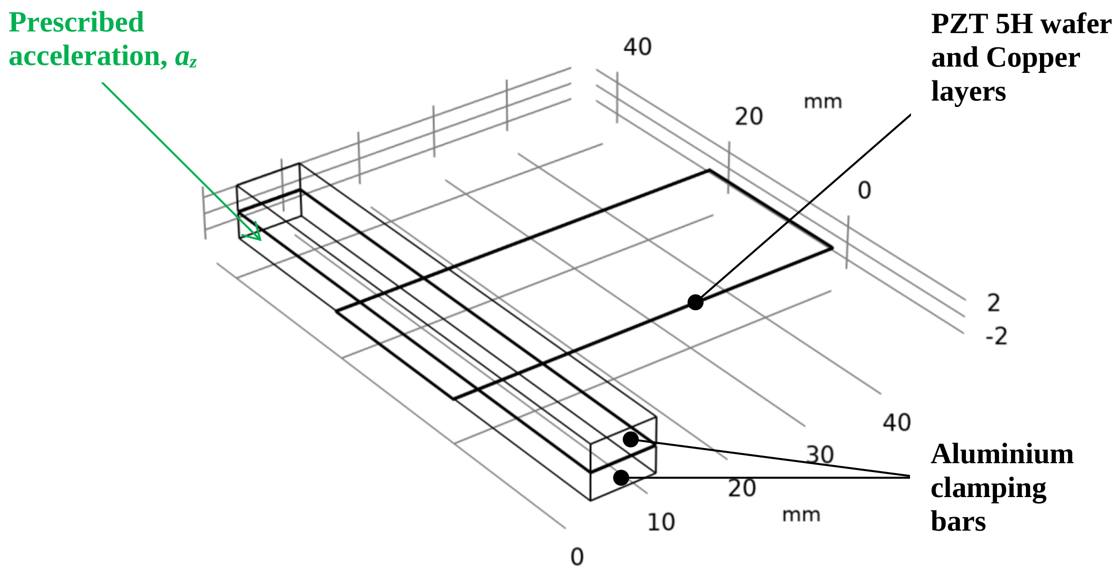

a) the entire domain.

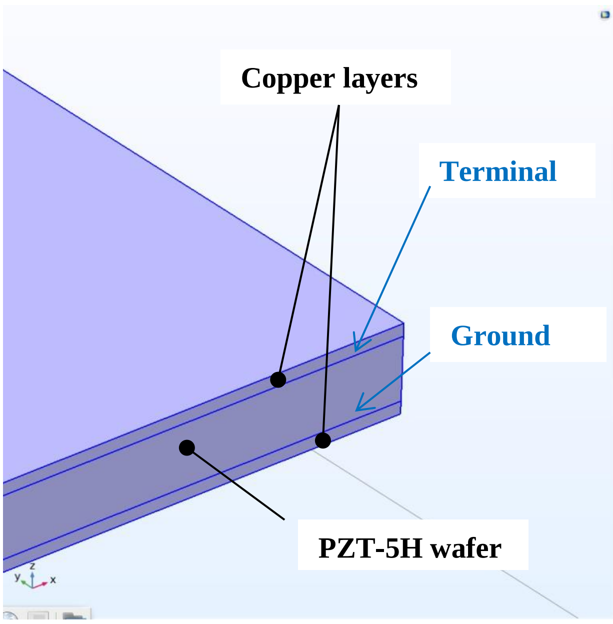

b) unimorph model.

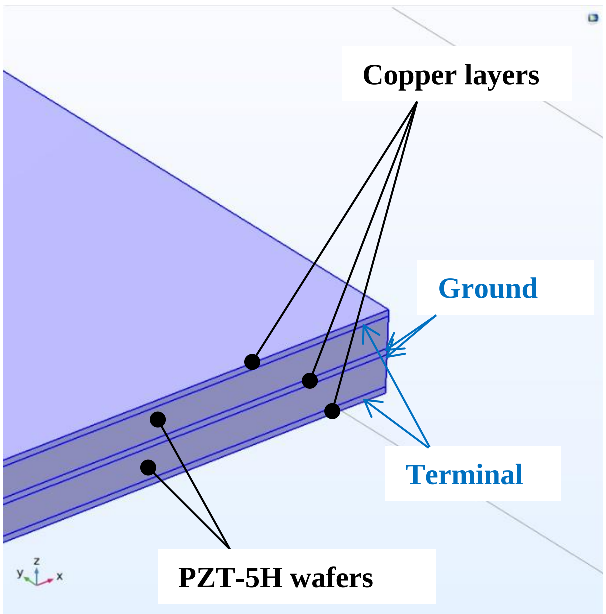

c) bimorph model.

Fig. 2 – The boundary conditions used for the Solid Mechanics and Electrostatics problem, and the constitutive parts of the two models.

The prescribed acceleration boundary condition applied at the bottom of the aluminum clamp (Fig. 2,a), for unimorph and bimorph harvesters, is given by a sinewave function as presented in the following sections.

A unimorph PEH (a single PZT-5H wafer) and a bimorph PEH (two PZT-5H wafers) were modelled. The dimensions of the wafers and the electric BCs are shown in Table 1.

Table 1

Layers dimensions and ground/terminal conditions considered for the unimorph, and bimorph PEH.

Unimorph PEH	**Bimorph PEH**	**Width**	**Depth**	**Height**	**z-axis offset**
Copper (GND)	Copper (Term)	49	20.8	0.003	0
PZT-5H	PZT-5H	49	20.8	0.015	0.003
Copper (Term)	Copper (GND)	49	20.8	0.003	0.018
	PZT-5H	49	20.8	0.015	0.021
	Copper (Term)	49	20.8	0.003	0.036

The dimensions are in millimetres. GND stands for ground, and Term is the terminal. For the bimorph PEH, ground condition is declared on both sides of the middle copper layer, corresponding to the inner faces of the two piezoelectric wafers. For the unimorph PEH the waveform acceleration applied on the bottom of the clamp (Fig. 2a) as BC is presented in Fig. 3.

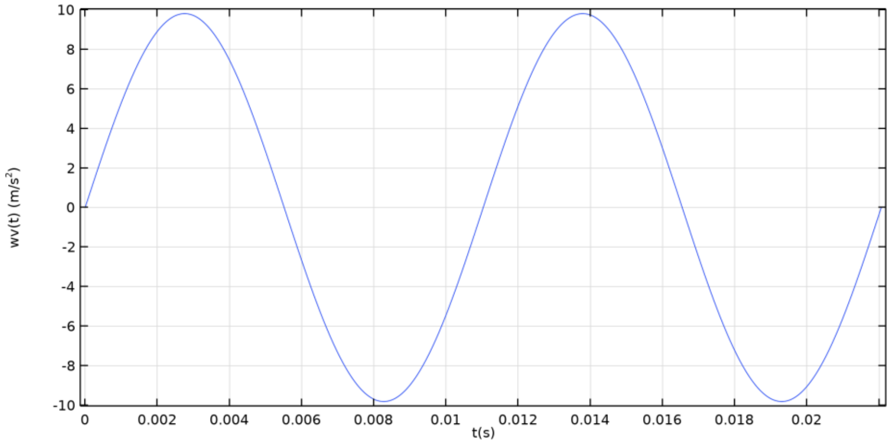

Fig. 3 – Input waveform for prescribed acceleration applied to unimorph model.

The sine waveform is applied only in the *z* direction; the period of the signal is according to the eigenfrequency, f_n = 90.656 Hz. The waveform sine acceleration for the bimorph PEH is presented in Fig. 4. The period of the signal coincides with the eigenfrequency of f_n =146.68 Hz found.

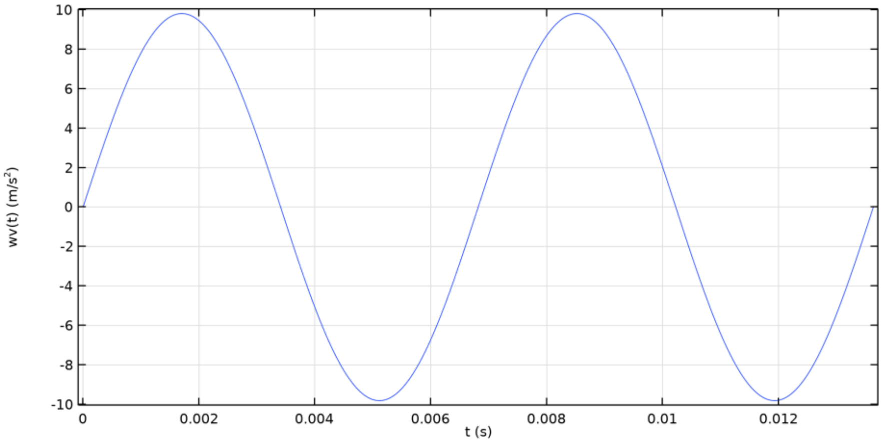

Fig. 4 – Input waveform for prescribed acceleration applied to bimorph model.

For both waveform signals from Fig. 3 and Fig. 4, the gravity acceleration gives the maximum amplitude, a = 9.81 m/s, in the z-direction.

3. SIMULATION RESULTS

Figure 5 presents the terminal voltage global evaluation of the unimorph cantilever when the quasi-stationary working condition is reached. The applied acceleration is at f_n = 90.656 Hz, and represented in Fig. 3. It is observed that the simulated PEH reaches a quasi-stationary regime after about 30 periods, which is quite in agreement with the time response in the experiments conducted on the quadmorph structure in our previous work [12].

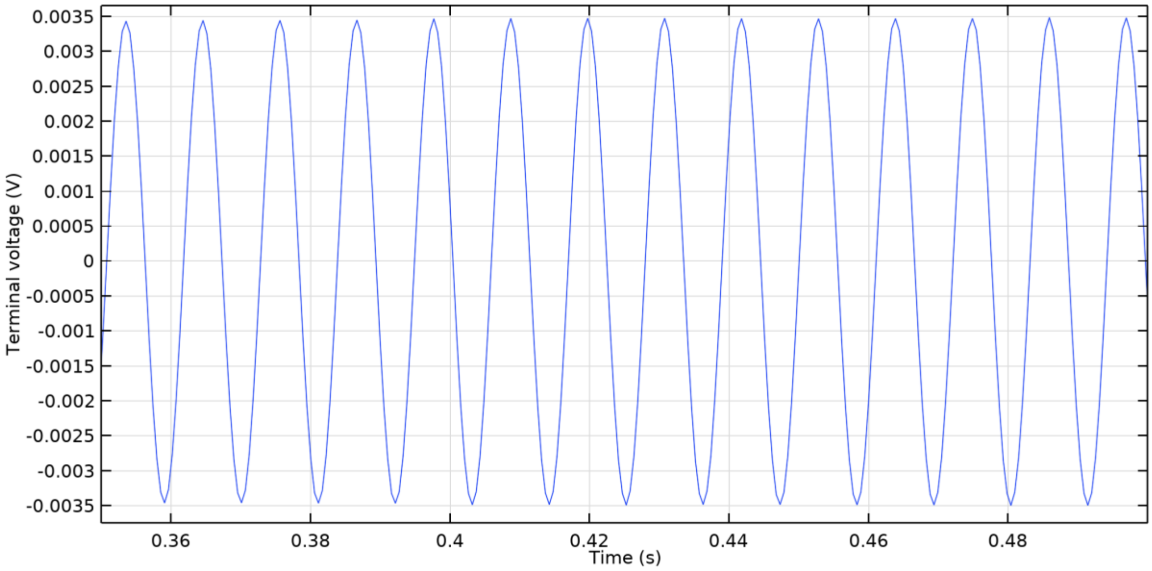

Fig. 5 – Terminal voltage rendered by the unimorph harvester in time domain.

Figure 6 shows the terminal voltage global evaluation of the bimorph structure for the last periods T_p, with T_p calculated as $1/f_n$, f_n = 146.68 Hz. The quasi-stationary working condition is reached after approximately 35 periods.

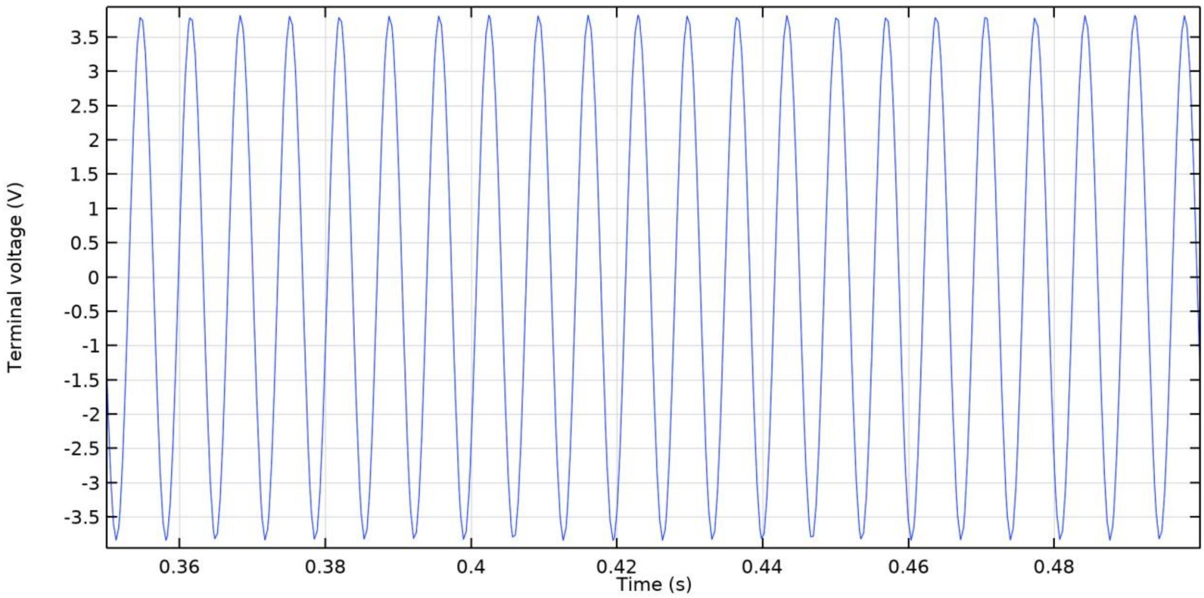

Fig. 6 – Terminal voltage output of the bimorph in a time-dependent study.

It is observed that the terminal voltage is improved to a great extent compared to the unimorph. Even if the two wafers would render double voltage output than the bimorph, what boosts the voltage from 7 mV together to more than 2 V is the positioning of the PZT-5H wafers. In unimorph case, the piezoelectric layer is in the middle, on the neutral fiber, which does not deform. Hence, the displacement is inferior, rendering a feeble electric response. In the case of the bimorph, the two PZT-5H wafers avoid the median line. This agrees with the Euler-Bernoulli beam theory [17].

The terminal voltage for the bimorph PEH from Fig. 6 is plotted considering the two wafers as independent. Future work will consider the two piezoelectric layers electrically connected in series so that the terminal voltage exhibits a more excellent value.

4. CONCLUSIONS

The paper aimed to assess the electric potentials rendered by a unimorph and a bimorph piezoelectric harvester in cantilever construction. Since the independent voltages of the layers cannot be observed experimentally, we conducted a series of finite element analyses to observe the electric outputs rendered unimorph and bimorph piezoelectric structures. The electric coupling of the PZT-5H wafers for the bimorph PEH is not considered, as the two wafers are electrically independent.

Future works will consider introducing an electric circuit node by adding an electric load. The study pursues evaluating the time response of the quadmorph structure (four PZT-5H wafers).

ACKNOWLEDGEMENTS

The acquisition of the quadmorph piezoelectric harvesters standing at the base of this research was funded by the Romanian Research and Development Institute for Gas Turbines COMOTI, on Nucleu project 11N/2017, PN 16.26.07.01. The simulations were conducted on the COMSOL Multiphysics server of the Laboratory of Energy Conversion and Sources, at the Faculty of Electrical Engineering, at the University POLITEHNICA of Bucharest.

The paper was presented at the Symposium of Electric Machines, SME'22, the XVIIIth edition.

REFERENCES

1. Y. Wang, Y. Lv, B. Lv, Y. Zhang, *Modeling, Simulation and analysis of intermediate fixed piezoelectric energy harvester*, Energies, **15**, *9*, p. 3294, 2022,
2. B. Debnath, R. Kumar, *A comparative simulation study of the different variations of PZT piezoelectric material by ising A MEMS vibration energy harvester*, IEEE Transactions on Industry Applications, **58**, *3*, pp. 3901–3908, 2022.
3. B. Sirisha, S. Chella, S. Sunithamani, M. Ravi Kumar, J. Lakshmi Prasanna, *Simulation and analysis of piezoelectric energy harvester with various proof-mass geometries*, International Journal of Online and Biomedical Engineering (iJOE), **18**, *07*, pp. 14–26, 2022.
4. S. Seok, A. Brenes, C. Yoo, E. Lefeuvre, *Experiment and analysis of a piezoelectric energy harvester based on combined FEM modeling and spice simulation*, Microsystem Technologies, **28**, *9*, pp. 2123–2130, 2022.
5. T. Jalabert, M. Pusty, M. Mouis, G. Ardila, *Investigation of the diameter-dependent piezoelectric response of semiconducting ZnO nanowires by Piezoresponse Force Microscopy and FEM simulations*, Nanotechnology, **34**, *11*, p. 115402, 2022.
6. R. R. Singh, D. Kumar, and M. Paswan, *numerical simulation of bimorph piezoelectric beam with circular holes*, Journal of The Institution of Engineers (India): Series D, 2022,
7. W. Mo, S. Huang, N. Liu, *Design and simulation of broadband piezoelectric energy harvester with multi-cantilever*, Proceedings of IncoME-VI and TEPEN, pp. 841–851, 2022.
8. H.Y. Wang, X. B. Shan, T. Xie, *Equivalent circuit simulation model of cantilevered piezoelectric bimorph energy harvester*, Applied Mechanics and Materials, **148–149**, pp. 245–249, 2011.
9. M. Reyaz Ahmad Vali, S. Faruque Ali, *Harvesting Energy from a Series of Harvesters*,

Recent Advances in Computational Mechanics and Simulations, pp. 573–585, 2020.
10. M.A. Bani-Hani, A.M. Almomani, K.F. Aljanaideh, S.A. Kouritem, *Mechanical modeling and numerical investigation of earthquake-induced structural vibration self-powered sensing device*, IEEE Sensors Journal, **22**, *20*, pp. 19237–19248, 2022.
11. Hosokawa, *Piezoelectric finite-difference time-domain simulations of piezoelectric signal generated in cancellous bone by ultrasound irradiation*, The Journal of the Acoustical Society of America, **152**, *4*, pp. A251–A251, 2022.
12. C. Săvescu, D. Comeagă, A. Morega, Y. Veli, *Experimental tests with piezoelectric harvester for tuning resonant frequency to vibrating source,* Revue Roumaine des Sciences Techniques, Série Électrotechnique et Énergétique, **67**, *4*, pp. 457–460, 2022.
13. C.I. Borzea, C.D. Comeagă, M.N. Uddin, R.D. Hrițcu, V.L. Ringheanu, *Improving the electric response of a cantilever piezoelectric energy harvester by constraining tip curvature*, IOP Conference Series: Materials Science and Engineering, **997**, p. 012038, 2020.
14. C. Borzea, D. Comeagă, A. Stoicescu, C. Nechifor, *Piezoelectric harvester performance analysis for vibrations harnessing*, U.P.B. Scientific Bulletin, Series C Electrical Engineering and Computer Science, **81**, *3*, pp. 237-248, 2019, ISSN 2286-3540.
15. Stoicescu, M. Deaconu, R.D. Hritcu, C.V. Nechifor, V.A. Vilag, *Vibration energy harvesting potential for turbomachinery applications*, INCAS Bulletin, **10**, *1*, pp. 135-148, 2018,
16. ***Midé Technology, PPA PRODUCTS Datasheet & User Manual, 2017. https://cdn2.hubspot.net/hubfs/3841176/Data-Sheets/ppa-piezo-product-datasheet.pdf.
17. C.I. Borzea, C.D. Comeagă, *Reliability of Euler-Bernoulli model for multilayer composite piezoelectric beams*, 11th International Symposium on Advanced Topics in Electrical Engineering (ATEE), 2019.
18. ***Comsol Multiphysics, v. 6.1.